Coded aperture correlation holography–a new type of incoherent digital holograms

A.Vijayakumar, [*] **Yuval Kashter, Roy Kelner, and Joseph Rosen**

Department of Electrical and Computer Engineering, Ben-Gurion University of the Negev, P.O. Box 653, Beer-Sheva 8410501, Israel
[*]*physics.vijay@gmail.com*

Abstract: We propose and demonstrate a new concept of incoherent digital holography termed coded aperture correlation holography (COACH). In COACH, the hologram of an object is formed by the interference of light diffracted from the object, with light diffracted from the same object, but that passes through a coded phase mask (CPM). Another hologram is recorded for a point object, under identical conditions and with the same CPM. This hologram is called the point spread function (PSF) hologram. The reconstructed image is obtained by correlating the object hologram with the PSF hologram. The image reconstruction of multiplane object using COACH was compared with that of other equivalent imaging systems, and has been found to possess a higher axial resolution compared to Fresnel incoherent correlation holography.

References and links

1. B. M. Oliver, "Sparkling spots and random diffraction," Proc. IEEE Lett. **51**(1), 220–221 (1963).
2. P. S. Considine, "Effects of Coherence on Imaging Systems," J. Opt. Soc. Am. **56**(8), 1001–1009 (1966).
3. J. P. Mills and B. J. Thompson, "Effect of aberrations and apodization on the performance of coherent optical systems. II. Imaging," J. Opt. Soc. Am. A **3**(5), 704–716 (1986).
4. J. B. Pawley, Handbook of biological and confocal microscopy, (Plenum, 1990) Chap. 1.
5. M. G. L. Gustafsson, "Surpassing the lateral resolution limit by a factor of two using structured illumination microscopy," J. Microsc. **198**(2), 82–87 (2000).
6. M. G. L. Gustafsson, D. A. Agard, and J. W. Sedat, "Sevenfold improvement of axial resolution in 3D wide-field microscopy using two objective lenses," Proc. SPIE **2412**, 147–156 (1995).
7. G. Indebetouw and P. Klysubun, "Imaging through scattering media with depth resolution by use of low-coherence gating in spatiotemporal digital holography," Opt. Lett. **25**(4), 212–214 (2000).
8. O. Mudanyali, D. Tseng, C. Oh, S. O. Isikman, I. Sencan, W. Bishara, C. Oztoprak, S. Seo, B. Khademhosseini, and A. Ozcan, "Compact, light-weight and cost-effective microscope based on lensless incoherent holography for telemedicine applications," Lab Chip **10**(11), 1417–1428 (2010).
9. J. Rosen and G. Brooker, "Digital spatially incoherent Fresnel holography," Opt. Lett. **32**(8), 912–914 (2007).
10. J. Rosen and G. Brooker, "Fluorescence incoherent color holography," Opt. Express **15**(5), 2244–2250 (2007).
11. J. Rosen, N. Siegel, and G. Brooker, "Theoretical and experimental demonstration of resolution beyond the Rayleigh limit by FINCH fluorescence microscopic imaging," Opt. Express **19**(27), 26249–26268 (2011).
12. J. Rosen and R. Kelner, "Modified Lagrange invariants and their role in determining transverse and axial imaging resolutions of self-interference incoherent holographic systems," Opt. Express **22**(23), 29048–29066 (2014).
13. R. Kelner, B. Katz, and J. Rosen, "Optical sectioning using a digital Fresnel incoherent-holography-based confocal imaging system," Optica **1**(2), 70–74 (2014).
14. R. Kelner and J. Rosen, "Parallel-mode scanning optical sectioning using digital Fresnel holography with three-wave interference phase-shifting," Opt. Express **24**(3), 2200–2214 (2016).
15. B. Javidi and T. Nomura, "Securing information by use of digital holography," Opt. Lett. **25**(1), 28–30 (2000).
16. E. Tajahuerce and B. Javidi, "Encrypting three-dimensional information with digital holography," Appl. Opt. **39**(35), 6595–6601 (2000).
17. S. Bernet, W. Harm, A. Jesacher, and M. Ritsch-Marte, "Lensless digital holography with diffuse illumination through a pseudo-random phase mask," Opt. Express **19**(25), 25113–25124 (2011).
18. A. Jesacher, W. Harm, S. Bernet, and M. Ritsch-Marte, "Quantitative single-shot imaging of complex objects using phase retrieval with a designed periphery," Opt. Express **20**(5), 5470–5480 (2012).

Corrected: 24 June 2016

19. T. Oshima, Y. Matsudo, T. Kakue, D. Arai, T. Shimobaba, and T. Ito, "Twin-image reduction method for in-line digital holography using periphery and random reference phase-shifting techniques," Opt. Commun. **350**, 270–275 (2015).
20. D. J. Goldstein, *Understanding the Light Microscope: A Computer Aided Introduction* (Academic, 1999) Chap. 1.
21. R. W. Gerchberg and W. O. Saxton, "A practical algorithm for the determination of phase from image and diffraction plane pictures," Optik (Stuttg.) **35**(2), 227–246 (1972).
22. G. Z. Yang, B. Z. Dong, B. Y. Gu, J. Y. Zhuang, and O. K. Ersoy, "Gerchberg-Saxton and Yang-Gu algorithms for phase retrieval in a nonunitary transform system: a comparison," Appl. Opt. **33**(2), 209–218 (1994).
23. G. Brooker, N. Siegel, V. Wang, and J. Rosen, "Optimal resolution in Fresnel incoherent correlation holographic fluorescence microscopy," Opt. Express **19**(6), 5047–5062 (2011).
24. M. K. Kim, "Adaptive optics by incoherent digital holography," Opt. Lett. **37**(13), 2694–2696 (2012).
25. P. Bouchal, J. Kapitán, R. Chmelík, and Z. Bouchal, "Point spread function and two-point resolution in Fresnel incoherent correlation holography," Opt. Express **19**(16), 15603–15620 (2011).
26. X. Lai, S. Xiao, Y. Guo, X. Lv, and S. Zeng, "Experimentally exploiting the violation of the Lagrange invariant for resolution improvement," Opt. Express **23**(24), 31408–31418 (2015).
27. M. K. Kim, "Full color natural light holographic camera," Opt. Express **21**(8), 9636–9642 (2013).
28. R. Kelner, J. Rosen, and G. Brooker, "Enhanced resolution in Fourier incoherent single channel holography (FISCH) with reduced optical path difference," Opt. Express **21**(17), 20131–20144 (2013).

1. Introduction

Optical imaging systems are commonly categorized into incoherent and coherent systems. Incoherent imaging systems may use low cost and eye safe light sources and do not suffer from speckle noise [1] and edge effects, unlike laser based coherent imaging systems [2,3]. Hence, incoherent imaging systems may be preferred over coherent systems for certain applications. Two important optical properties of imaging systems are the lateral and axial resolutions governed by the numerical aperture (NA) and the wavelength λ of the source by the relations $0.61\lambda/NA$ and $2\lambda/(NA)^2$, respectively [4]. Different techniques have been developed to enhance the lateral [5] and axial resolution [6] of imaging systems.

Incoherent digital holography systems have been found useful for various tasks and applications of microscopy [7,8]. A self-informative-reference holographic technique dubbed Fresnel incoherent correlation holography (FINCH) was invented in 2007 [9,10]. FINCH exhibits a modulation transfer function (MTF) whose width is twice of that of any coherent imaging system with the same NA and, unlike regular imaging systems, has a uniform response to all the frequencies below the cutoff frequency [11]. This unusual MTF profile enables FINCH to break the classical limits and achieve a resolving power, which is roughly 1.5 times and 2 times that of equivalent incoherent and coherent imaging systems, respectively. However, a careful analysis of the axial behavior of FINCH leads to the conclusion that FINCH has a low axial resolution in comparison to regular imaging systems [12].

Lately, a sectioning-capable FINCH configuration was proposed; a scanning phase pinhole is used to suppress out-of-focus information and achieve better axial resolution [13]. However, the information acquisition is time consuming when only a single phase pinhole is used. To achieve optical sectioning in less time, parallel scanning using multiple pinholes is suggested [14]. Still, in addition to the longer acquisition time, the optical sectioning FINCH configurations require two spatial light modulators (SLMs).

In this study, we propose a new incoherent self-informative-reference digital holography system with an improved axial resolution dubbed coded aperture correlation holography (COACH). Phase masks functioning as random apertures have been used in coherent processors to serve different purposes such as security [15] and encryption [16]; they can also be used as diffusers for artifacts and twin image reduction [17–19]. To the best of our knowledge, this is the first time that random-like phase masks are utilized as coded apertures in incoherent holography systems. Note, however, that the use of random phase masks is not uncommon in coherent optics [15–19].

In COACH, a coded phase mask (CPM) acts as an axial resolution enhancer by constricting the hologram reconstruction depth of focus to a narrower axial region than of FINCH. In addition, since the CPM has a random-like nature, the acquired holograms are encrypted, in the sense that in order to reconstruct the image of the recorded object, the CPM

values are required. Thus, the proposed system offers a new method of three-dimensional (3D) holographic encryption for incoherently illuminated, or self-luminous, objects.

2. Methodology

In the proposed system, at least two holograms are recorded under identical conditions, with the same CPM: one hologram called as the object hologram contains the information of the object under observation; another is recorded using a point source, called as the point spread function (PSF) hologram. The image of the object is reconstructed by correlating the complex PSF hologram, with the complex object hologram. Due to the randomness-like nature of the phase mask, a deviation of more than the correlation length [15,16] in the axial distance of the pinhole, or of the object, distorts the reconstructed image significantly, resulting in a rapid fall of intensity of the reconstructed image. Therefore, to image a thick object using COACH, a library of PSF holograms should be recorded in order to reconstruct the object hologram at different planes. In other words, the COACH system should go through a stage of coaching, in which a library of PSF holograms for the various planes along the z axis are acquired, enabling reconstruction of the single object hologram at these planes in the stage of object recovery.

The optical configuration of COACH is shown in Fig. 1. Light from an incoherent light source is focused by the lens L_1 onto an object in a critical illumination configuration [20]. Assuming the light source is quasi-monochromatic and spatially incoherent, the light emitted by each object point is coherent only with itself. Therefore, every two beams originating from the same object point are coherently interfered, encoding the information of the intensity and the location of the particular object point. The light diffracted by the object point is collected and collimated by the lens L_2. The collimated light is polarized by the polarizer P_1 to an orientation of 45° with respect to the active axis of the SLM. A random-like phase profile, constituting the CPM, is displayed on the phase-only SLM. The CPM is calculated using the Gerchberg-Saxton (G-S) algorithm to obtain uniform intensity in the spectrum domain [21,22]. Therefore, in both domains, in the CPM and in its spatial spectrum, the functions are projected every iteration by the G-S algorithm into the constraint group of pure phase functions. As the polarization of the collimated light is oriented at 45° with respect to the active axis of the SLM, only about half the intensity of the incident light is modulated by the CPM, while the remaining half traverses without any modulation. A second polarizer P_2, with an orientation of 45° with respect to the active axis of the SLM, is mounted after the SLM to allow the propagation of only identically oriented components of the modulated and unmodulated waves to create interference between them at the sensor plane. The above polarization multiplexing scheme creates a compact, single channel optical configuration [23]. A phase shifting procedure, similar to [9], is used, where three holograms corresponding to three phase values of $\theta = 0°$, 120°, and 240° are recorded and are superposed to cancel the twin image and the zeroth order terms. The complex hologram for the pinhole object is the PSF hologram H_{PSF} [24]. The pinhole is then replaced by an object at the exact axial location and a hologram H_{object} is recorded with identical conditions. The H_{PSF} and H_{object}, when correlated, yield the reconstructed image at the plane of the pinhole.

Although the configuration of a lens, polarizers, an SLM and an image sensor is similar in structure to that of FINCH [23], there are fundamental differences in the type of the recorded holograms and in the PSF of each system, as is shown in the following. Consequently, the imaging features of the two systems are also different. The hologram of FINCH is a superposition of shifted and scaled quadratic phase functions, whereas the hologram of COACH is a superposition of shifted random-like, complex-valued, functions (dubbed herein as PSFs). Consequently, the way of recording and reconstructing holograms, and the image resolutions (axial and lateral) are all completely different between these two systems. COACH holograms cannot be merely classified into the categories of Fresnel, Fourier or image holograms. Moreover, FINCH and other self-informative-reference holographic techniques first duplicate the object into two images that are mutually interfered on the sensor plane. COACH, on the other hand, does not duplicate the image at all. Instead, the object is

imaged only once and the image is interfered with a quasi-random distributed wavefront on the sensor plane. In this sense, COACH is a change of concept from the traditional self-informative-reference incoherent hologram recorders. Nevertheless, the fact that FINCH and COACH are implemented by the same optical system suggests that one can record both holograms by only displaying different CPMs on the SLM; by doing that, the different benefits of both hologram types can be gained.
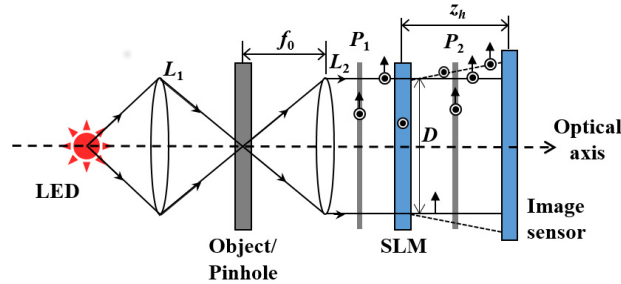

Fig. 1. COACH configuration for recording object and PSF holograms.

The following analysis of COACH is based on the scheme of Fig. 1. The pinhole at the axes origin induces on the sensor plane two interfering beams, one is a plane wave (in which its polarization, before P_2, is oriented in parallel to the plane of the page) with amplitude A, and a random-like complex function $G(u,v)$ (in which its polarization, before P_2, is oriented vertically to the plane of the page). The function $G(u,v)$ is the complex amplitude obtained after free-space propagation from the CPM, displayed on the SLM, along a distance z_h to the sensor plane. According to the analysis below, the PSF hologram H_{PSF} is equal to $G(u,v)$. To minimize the reconstruction background noise, it is suggested to force, as much as possible, a uniform magnitude on the spatial spectrum of the CPM. The reason for that can be understood by looking on $H_{PSF} = G(u,v)$. Assuming the magnitude of H_{PSF} spectrum is also approximately uniform, the reconstructed image of a point, obtained by autocorrelation of H_{PSF}, is nearly the sharpest with minimum side-lobes. To force the uniformity on the magnitude of the spatial spectrum, the CPM function $\exp[i\varphi(x_p,y_p)]$ is synthesized by the G-S algorithm, whereas the constraint at the spectral domain is a uniform magnitude and the constraint on the SLM plane is to have a pure phase function. The SLM pixels are used as the degrees of freedom for the G-S algorithm. Therefore, more pixels mean that the magnitude of H_{PSF} spectrum is more uniform and the background noise is expected to be lower. Thus, the reconstruction noise level is dependent on the status of the SLM technology, in the sense that higher density SLMs are expected to yield COACH with less noise.

The resulting CPM from the G-S algorithm is displayed on the SLM three times, each of which with a different phase constant. Hence, the intensity distribution recorded by the image sensor is:

$$I_k(u,v) = \left| A + G(u,v)\exp(i\theta_k) \right|^2, \qquad k = 1, 2, 3, \tag{1}$$

where θ_k is the kth phase value used for the phase shifting procedure. Following this procedure, the complex hologram obtained for the point source is $A*G(u,v)$. Thus, $H_{PSF} = G(u,v)$ is the PSF of the COACH, or, in other words, $G(u,v)$ is the reconstructing function of the entire holograms of arbitrary two-dimensional (2D) objects placed at the same transverse plane of the pinhole.

An arbitrary 2D, incoherently illuminated object $t(x,y)$ can be represented as a collection of uncorrelated radiating points as follows:

$$t(x,y) = \sum_j a_j \delta(x - x_j, y - y_j). \tag{2}$$

Assume that the object is located at the same distance f_0 as the pinhole, where f_0 is the focal length of L_2. Each source point j induces two mutually coherent beams on the sensor plane: one is a tilted plane wave of the form $A_j\exp[i2\pi(ux_j + vy_j)/\lambda f_o]$; the other is a shifted version of $G(u,v)$ multiplied by the same plane wave, where λ is the central wavelength. Formally, this beam can be represented as $\exp[i2\pi(ux_j + vy_j)/\lambda f_o]G(u-u_j,v-v_j)$, where $(u_j,v_j) = (x_j,y_j)z_h/f_o$. Consequently, the overall intensity distribution on the sensor plane, due to the entire object, is

$$I_k(u,v) = \sum_j \left| A_j \exp\left[\frac{i2\pi(x_j u + y_j v)}{\lambda f_o}\right] + \exp(i\theta_k) B_j \exp\left[\frac{i2\pi(x_j u + y_j v)}{\lambda f_o}\right] G(u-u_j, v-v_j)\right|^2.$$

(3)

The complex hologram can be synthesized from the three exposures $I_{k=1,2,3}$ as shown below:

$$H(u,v) = I_1(u,v)\left[\exp(-i\theta_3) - \exp(-i\theta_2)\right]$$
$$+ I_2(u,v)\left[\exp(-i\theta_1) - \exp(-i\theta_3)\right] + I_3(u,v)\left[\exp(-i\theta_2) - \exp(-i\theta_1)\right].$$

(4)

The complex hologram obtained from the phase shifting procedure, following Eq. (4), is

$$H(u,v) = \sum_j A_j^* B_j G(u-u_j, v-v_j).$$

(5)

The image reconstruction is carried out by correlating the complex PSF hologram $H_{PSF} = G(u,v)$ and the complex object hologram as follows:

$$P(u',v') = \iint \left\{\sum_j A_j^* B_j G(u-u_j, v-v_j)\right\} G^*(u-u', v-v') \, du \, dv$$
$$\approx \sum_j A_j^* B_j \delta(u'-u_j, v'-v_j) \propto t(u'/M_T, v'/M_T),$$

(6)

where integration over different wavelengths can be avoided under the assumption of quasi-monochromatic light.

The resulting image is indeed a magnified version of the object, with transverse magnification of $M_T = z_h/f_o$. Since the image is obtained via correlation, the minimal size of a resolved image details is nearly equal to the correlation length, determined by half of the width of the smallest spot that can be recorded on the sensor plane by the SLM with a diameter of D. Based on diffraction considerations, the width of the smallest spot on the sensor plane is approximately $2.44\lambda z_h/D$. When the resolution limit is projected to the object space, the minimal resolved size in the object is approximately $1.22\lambda f_o/D$, which is about the same resolution limit of a regular incoherent imaging system with a similar NA. It is interesting to note that unlike other incoherent self-informative-reference digital holographic systems {e.g., FINCH [12,25,26], self-interference incoherent digital holography (SIDH) [27] and Fourier incoherent single channel holography (FISCH) [28]}, COACH always satisfies the well-known Lagrange invariant. In this sense, COACH is unique, but inherently it lacks the superior transverse resolving power that the above mentioned systems have.

The axial resolution of COACH is dictated by the longitudinal correlation length, determined by the axial size of the smallest spot that can be recorded on the sensor plane using an SLM with an aperture of diameter D. Based on the diffraction theory, this axial size is approximately $16\lambda(z_h/D)^2$. When this figure is projected to the input space, the minimum resolved axial size in the object is $8\lambda(f_o/D)^2 = 2\lambda/(NA)^2$, which is about the same resolution limit of a conventional imager [4]. To conclude the analysis part, COACH is expected to possess similar lateral and axial resolution capabilities of a conventional imaging system, but with the advantage of storing a 3D image in a single 2D hologram. It should be emphasized that, just like in conventional holography, this does not imply that the entire 3D internal

structure of the object is retrieved. In comparison to FINCH, the transverse resolution capability of COACH is inferior, while its axial resolution is superior.

3. Experiments

The principle of COACH is experimentally demonstrated using the digital holographic setup shown in Fig. 2. Two light emitting diodes (LEDs) (Thorlabs LED631E, 4 mW, λ = 635 nm, $\Delta\lambda$ = 10 nm) are mounted on the two illumination channels. Two identical lenses L_{1A} and L_{1B}, denoting a lens system comprising an objective lens and a convex lens with effective focal length values of 3 cm and 7 cm, were mounted in the channel 1 and channel 2, respectively, to critically illuminate the objects [20]. Two identical irises with a radius of 0.6 cm were mounted on both channels immediately after the lenses L_{1A} and L_{1B} to control the NA of the critical illumination. The distance between the iris and the object was 15 cm, imposing an NA of 0.04. Hence, the lateral resolution is roughly 10 μm (0.61λ/NA) and the axial resolution is about 0.8 mm [2λ/(NA)^2]. Negative National Bureau of Standards chart (NBS) (NBS 1963A Thorlabs) and United States Air Force chart (USAF) (USAF 1951 1X Edmund Optics) charts were mounted in channel 1 and channel 2, respectively. Element 7.1 lp/mm of NBS chart and elements 2 (4.49 lp/mm) and 3 (5.04 lp/mm) of group 2 in USAF chart were illuminated. A pinhole with a size of approximately 100 μm was used as the point object. The light diffracted by the objects (USAF and NBS charts) was incident on lens L_2 with a focal length of f_0 = 20 cm, placed at a distance of 20 cm from the two objects. The light collimated by the lens L_2 is polarized by the polarizer P_1 oriented to an angle of 45° with respect to the active axis of SLM (Holoeye PLUTO, 1920 × 1080 pixels, 8 μm pixel pitch, phase-only modulation). A CPM calculated using G-S algorithm was displayed on the SLM using 1080 × 1080 pixels. About half of the intensity of light is modulated by the CPM while the remaining propagates as an unaffected beam. As per the phase shifting method, three CPMs corresponding to θ = 0°, 120° and 240° were displayed in the SLM for eliminating the twin image and the zeroth order terms.
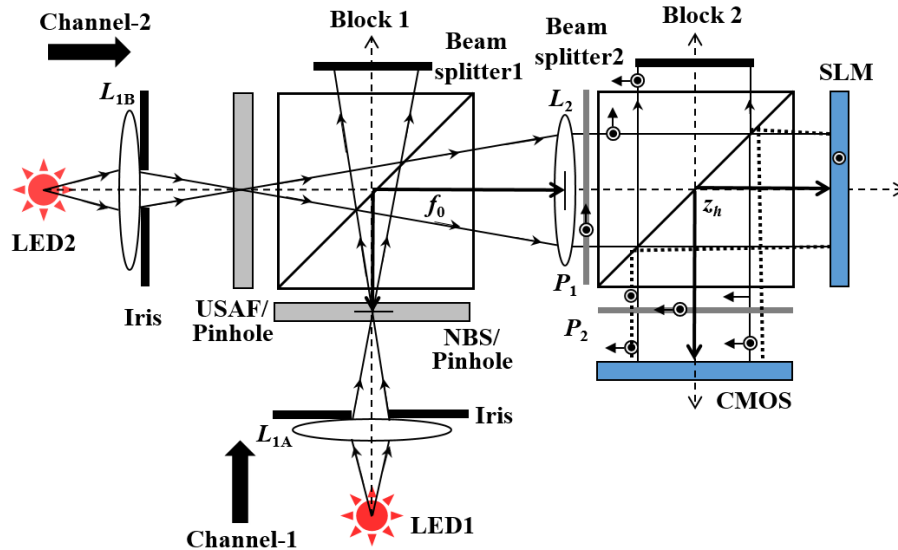

Fig. 2. Experimental setup of COACH with two illumination channels.

The distance between L_2 and the SLM was 11 cm. The distance between the SLM and the second beam splitter was 5 cm. A polarizer P_2, oriented at 90° with respect to the orientation of P_1, was used to only allow components of the modulated and unmodulated light (from SLM) with same orientation, to enable interference between them on the camera (Hamamatsu ORCA-Flash4.0 V2 Digital CMOS, 2048 × 2048 pixels, 6.5 μm pixel pitch, monochrome).

The distance between the SLM and the camera was $z_h = 15$ cm. The targets were aligned such that the elements 7.1 lp/mm of the NBS chart and elements 2 and 3 of group 2 in USAF chart can be imaged onto the camera. The object holograms H_{object} for the three phase shift values were recorded and superposed [9]. Similarly, PSF holograms H_{PSF} with three phase shift values were recorded by replacing the USAF or the NBS with the pinhole and blocking the other channel. The pinhole was located on the optical axis [i.e., with $(x,y) = (0,0)$] at the same distance as the object from L_2. Due to the shift-invariance property of the system, as reflected by Eq. (6), the pinhole can be shifted to various (x,y) locations, away from the optical axis, in the limits of the system field-of-view, without distorting the reconstruction. The image was reconstructed by correlating H_{object} with H_{PSF}.

In the first experiment, the hologram of an element of the NBS chart and a hologram of the pinhole were recorded using the COACH principle, both with the same CPM and at the same axial location. The NBS chart was reconstructed by correlating H_{PSF} and H_{object}, as shown in Fig. 3. The holograms of the pinhole and NBS chart for the three phase-shift values are shown in Figs. 3(a)–3(c) and Figs. 3(d)–3(f), respectively. The magnitude of the complex holograms of the pinhole and NBS chart are shown in Figs. 3(g) and 3(h), respectively. The phase of the complex holograms of the pinhole and NBS chart are shown in Figs. 3(j) and 3(k), respectively. The phase image of the CPM is shown in Fig. 3(i) and the reconstruction result is shown in Fig. 3(l).
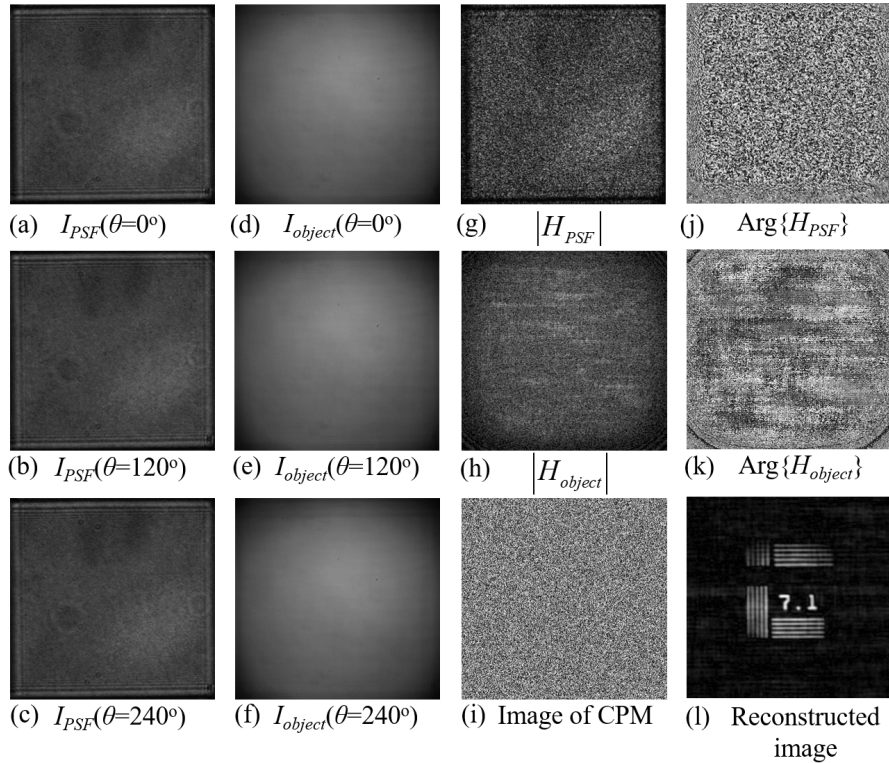
(a) $I_{PSF}(\theta=0^\circ)$	(d) $I_{object}(\theta=0^\circ)$	(g) $\left	H_{PSF} \right	$	(j) Arg$\{H_{PSF}\}$
(b) $I_{PSF}(\theta=120^\circ)$	(e) $I_{object}(\theta=120^\circ)$	(h) $\left	H_{object} \right	$	(k) Arg$\{H_{object}\}$
(c) $I_{PSF}(\theta=240^\circ)$	(f) $I_{object}(\theta=240^\circ)$	(i) Image of CPM	(l) Reconstructed image

Fig. 3. (a)–(c) PSF holograms with phase shift values of 0°, 120° and 240°, respectively; (d)–(f) object holograms with phase shift values of 0°, 120° and 240°, respectively; (g) and (h) magnitude of the complex hologram of the pinhole and the NBS chart; (i) phase image of the CPM; (j) and (k) phase of the complex hologram of the pinhole and the NBS chart; and (l) result of the reconstruction by correlating the complex PSF with the object hologram.

In the next experiment, the axial resolution of the three systems, namely regular imaging, FINCH, and COACH, were compared by the following experiment. For COACH, the axial location of the pinhole was varied and corresponding H_{PSF}s were recorded, for every location

of the pinhole. The recorded H_{PSF}s were correlated with the H_{PSF} recorded when the pinhole was located at the front focal plane of lens L_2. The intensity of the reconstructed image at $(x,y) = (0,0)$ was plotted against the location of the pinhole. A similar experiment was carried out for FINCH by recording the FINCH hologram of the pinhole at different axial locations and reconstructing the image using Fresnel back propagation [9, 12], with the reconstructing distance corresponding to the plane where the pinhole is at the front focal plane of lens L_2. The location of the pinhole was varied again and the image of the pinhole at the constant sensor plane, for every axial location, was recorded in the case of regular imaging. In other words, the image intensity at $(x,y) = (0,0)$ was measured for every input plane to understand how rapidly the out of plane information is defocused. The plots of the intensity values of reconstruction/imaging at $(x,y) = (0,0)$ for the above three systems are shown in Fig. 4. The depth of field of the COACH system matches very well with the regular imaging, indicating that their axial resolutions are the same, while FINCH exhibits an inferior axial resolution, as described in our earlier studies [12].
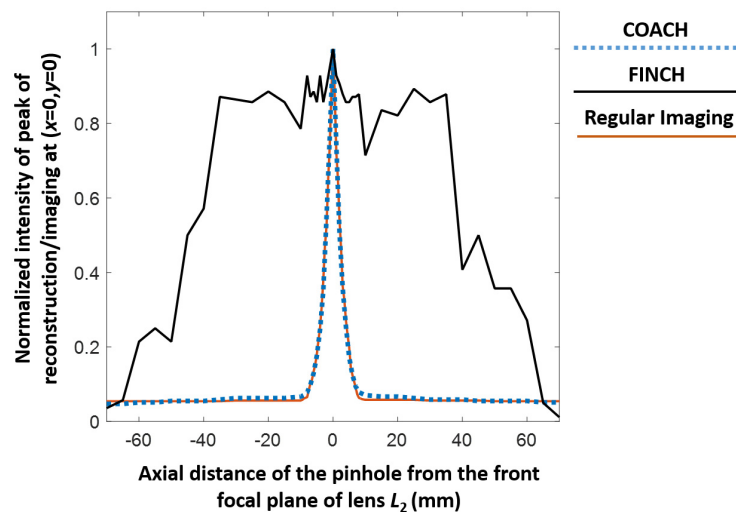

Fig. 4. Normalized intensity of reconstruction/imaging at $(x = 0, y = 0)$ versus the axial distance of the pinhole from the front focal plane of lens L_2.

In order to experimentally analyze further the axial resolution of COACH in a practical scenario, two planar objects were constructed using the NBS and USAF resolution charts mounted onto channels 1 and 2, respectively, at different relative distances. During the experiment, the location of the USAF chart in channel 2 had been modified, while the location of NBS chart in channel 1 had been kept constant; the relative distance (Δd) between the NBS chart and USAF chart had been varied from −3 cm to 3 cm, in steps of 1 cm. Besides recording H_{object}, H_{PSF} was recorded at every axial location of the USAF chart, in order to enable reconstruction of the object at these different planes. The experiment is equivalent to recording a thick object whose thickness is varied from 0 cm to 3 cm, while any axial plane can be reconstructed using H_{PSF} recorded at the same plane. In order to evaluate COACH, FINCH holograms, as well as regular images, were recorded in the same configuration of the NBS and USAF charts. The FINCH configuration is similar to the setup of [9] (but employs the polarization method [23]), in which the PSF is obtained from an interference between converging spherical and plane waves. The focal lengths of the diffractive lens displayed on the SLM for regular imaging and for recording FINCH holograms, when the objects are located at the front focal plane of lens L_2, are 14.2 cm and 35 cm, respectively. The reconstruction distance for FINCH was $z_r = -19.8$ cm. The regular images, FINCH, and

COACH reconstructions of the thick object, at the two different in-focus planes, are given in Fig. 5.
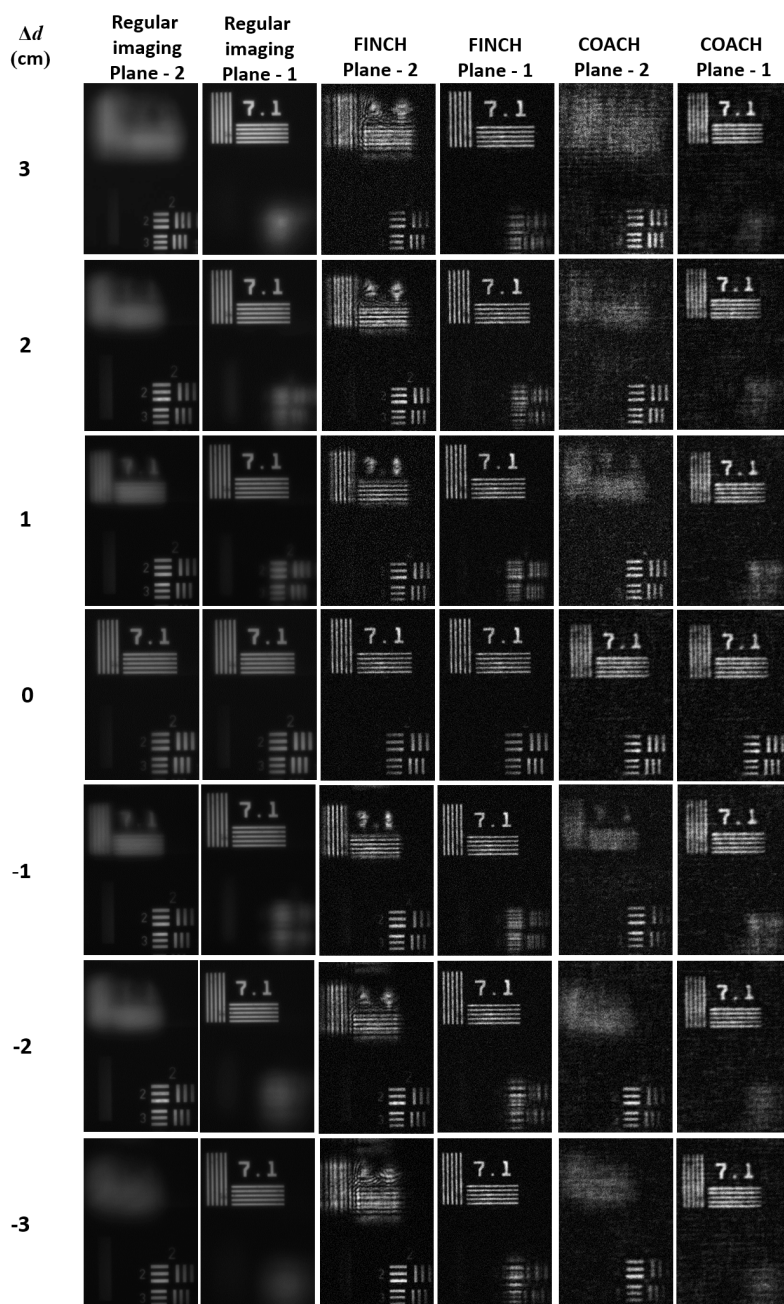

Fig. 5. Experimental comparison results of regular imaging and reconstruction of the FINCH and COACH holograms at plane 1 (NBS chart) and plane 2 (USAF chart) of channels 1 and 2 respectively, when the location (Δd) of the USAF chart relative to NBS chart was varied from −3 cm to 3 cm in steps of 1 cm.

It can be noted that FINCH demonstrates a low axial resolution, as expected from the previous analyses [12]. The out-of-focus images of FINCH in the third and fourth columns are more intense than of COACH and the regular imager, even for axial shifts of ± 3 cm.

COACH, on the other hand, shows a higher axial resolution, when compared with FINCH, and similar performance, when compared with regular imaging. The out-of-focus images of COACH in the fifth and sixth columns are weaker than of FINCH for axial shifts of only ± 1 cm. However, based on Fig. 5, it is also noted that COACH possesses a higher level of background noise when compared with the other imagers. The average standard deviation of the background noise was found to be 2×10^{-5}, 2.3×10^{-4} and 1.7×10^{-3} for normalized images of regular imaging, FINCH and COACH, respectively. The standard deviation of COACH is found to be two and one orders of magnitude higher than that of regular imaging and FINCH, respectively.
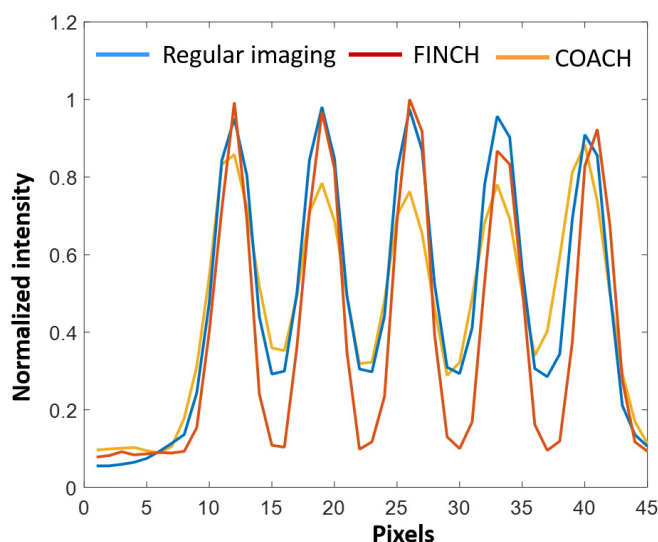

Fig. 6. Average cross-sections of the 7.1 lp/mm gratings calculated based on regular imaging and on the reconstructions of FINCH and COACH acquired holograms.

Average cross-sections of the 7.1 lp/mm gratings calculated based on regular imaging and on the reconstructions of FINCH and COACH acquired holograms are shown in Fig. 6. The visibility of the gratings was found to be 0.54, 0.81 and 0.43 for regular imaging, FINCH and COACH respectively, demonstrating the higher lateral resolution of FINCH as was reported earlier in [11, 12].

The concept of COACH is demonstrated in this study with an emphasis on the axial resolution enhancement over FINCH, where the reconstruction of different planes was carried out using H_{PSF} recorded at a single plane and the degree of defocusing is demonstrated. However, the same technique can also be used for information concealment [15, 16], where the information in each plane of the object can be unlocked by using the appropriate keys, which are the PSF holograms recorded at these planes with different CPMs. The feature of information concealment by COACH is demonstrated in Fig. 7. Two holograms of the same object, located at the same plane, were captured using two different CPMs. With these exactly two CPMs, two different holograms of the same pinhole, located at the same plane of the object, were recorded. Following the phase shifting procedure, there were two different reconstructing PSFs for the two object holograms. The reconstruction results of the two object holograms, by a correlation with the two reconstructing PSFs, are shown in Fig. 7. From Fig. 7, it is clear that only the reconstruction of a hologram by its corresponding PSF, both recorded with the same CPM, can recover the image of the original object. Correlating a hologram, recorded using one CPM, with a PSF, recorded using a different CPM, yields a blur, meaningless distribution.
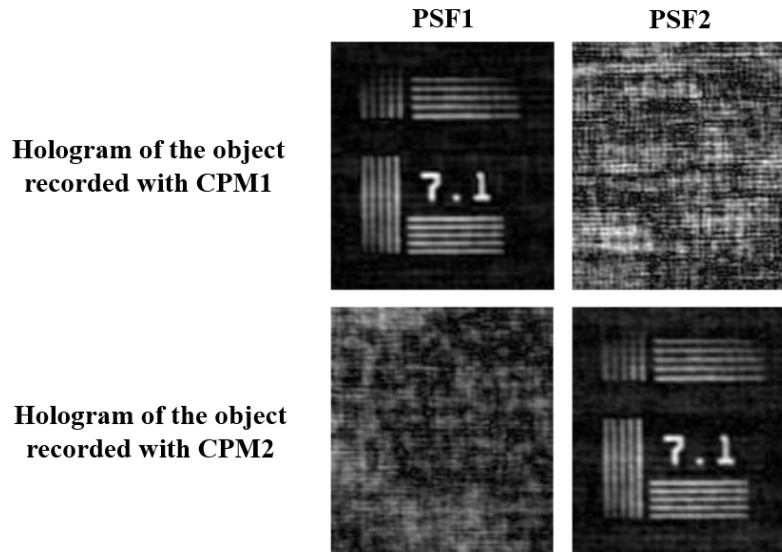
Fig. 7. Experimental results presenting reconstructions of two COACH holograms each recorded with a different CPM. For each CPM, a corresponding PSF hologram was also recorded. The reconstructions were performed by correlating each hologram with each of the two PSFs holograms. Only the reconstruction of a hologram with its corresponding PSF, both originated from the same CPM, yields a proper image of the recorded object.

4. Summary and conclusions

In conclusion, we have proposed and demonstrated COACH, a new digital incoherent holographic system that possesses higher axial resolving power compared to FINCH. COACH is actually a generalized incoherent digital hologram recorder, in the sense that FINCH [9–11, 23] and SIDH [27] are special cases of COACH, in which the CPM is a quadratic phase function, rather than the almost arbitrary CPM used for COACH. However, whereas these special cases can violate the Lagrange invariant, COACH, in the presented case, does not. The reason that COACH satisfies the Lagrange invariant but FINCH might violate it, is because in FINCH, the hologram is recorded as an interference between two images of the same object (in some cases one of the images is obtained at infinity), whereas, in COACH, the hologram is recorded as an interference between a single image of the object (located at infinity) with a quasi-random distributed beam. Looking at an object point located at some transverse distance from the origin, in FINCH, this point is first imaged into two point images at different axial locations. The transverse distance of the two image points from the origin is expressed by linear phases that each image point projects on the sensor plane. When these two linear phases constructively interfere, the distance from the origin of the final reconstructed image point is doubled, without any change in the size of the reconstructed spot itself. The overall effect is that the transverse image magnification is as twice as the spot magnification. This inequality of the magnifications is actually the manifestation of the violation of the Lagrange invariant [12]. On the other hand, since in COACH, the camera observes only on a single image (usually, and in this study, the image is at infinity) there is no occasion of a constructive interference between two linear phases on the camera plane. Hence, the transverse magnification is always equal to the spot magnification. This equality between the two magnifications is one of the manifestation of the Lagrange invariant [12]. Consider Eq. (3), one can see that for every point j there are two linear phases with the same sign in the two terms. When one opens the brackets, the cross terms are left without any linear phase - the linear phases have been vanished as a result of a mutual cancelation. In FINCH, on the other hand, the two linear phases can appear with opposite sign (See for example Eq. (24) in Ref [12].) and therefore the cross terms have linear phases with a factor maximally

two times bigger than the original factor. The practical consequence of this feature is that COACH has resolution limits of conventional imagers. Even though COACH has higher axial resolution than FINCH, its lateral resolution is lower than that of the optimal FINCH [11].

In this optical configuration of COACH, a tolerance of about 1 mm was noted in the distance of recording the PSF and the object holograms. Beyond 1 mm the image was blurred, while within 1 mm the variation in reconstruction was minor. This tolerance range matches to the theoretical estimation of axial resolution distance of 0.8 mm and also the graph shown in Fig. 4. Thus, we believe that COACH can be utilized for high sensitivity imaging systems and microscopes for the analysis of thick objects. Specifically, COACH can be implemented in 3D fluorescence microscopes in a similar fashion to FINCH [10,11,23]. However, due to the better axial resolution of COACH, it is expected that out-of-focus objects will not disturb as much as in a FINCH microscope.

For studying thick objects using COACH, a library of PSF holograms can be recorded, and the different planes of the object, corresponding to the planes of recording PSF holograms, can be effectively reconstructed. It should be noted that COACH requires the recording of PSF holograms at different planes, which may require a mechanical axial scanning system. However, the recording of PSF holograms at various planes is necessary only once. Once a library of PSF holograms is created off-line and stored in a computer along with the CPM information, it can be reused on-line as many times to view any thick object in a motionless manner. On the semantic side, the process of acquiring PSFs can be viewed as coaching the system, thus giving the acronym COACH additional meaning.

Acknowledgment